Experimental Verification of Z Antennas at UHF Frequencies

Richard W. Ziolkowski, *Fellow, IEEE*, Peng Jin, *Student Member, IEEE*, J. A. Nielsen, M. H. Tanielian, and Christopher L. Holloway, *Senior Member, IEEE*

***Abstract*—Both 300- and 570-MHz versions of an electrically small, coaxially fed Z antenna were designed and tested. These two cases demonstrate the ability to change the resonance frequency of the Z antenna by changing the value of its lumped element inductor. The numerically predicted and measured results are in good agreement.**

***Index Terms*—Antenna efficiency, antenna theory, electrically small antennas (ESAs), metamaterials, parasitics, quality factors.**

I. Introduction

THE proliferation of wireless devices for communication and sensor applications has restimulated interest in efficient, broad-bandwidth, easy-to-build, and inexpensive electrically small antennas (ESAs). These often conflicting requirements have made the design tasks onerous for antenna engineers with traditional schemes. Several metamaterial-inspired antennas proposed recently [1], [2] have provided an alternative ESA design paradigm to address such issues. The performance characteristics of the 3D magnetic EZ antenna proposed in [2] have been recently verified experimentally [3]. The Z antenna, a variant of the 2D electric EZ antenna that was introduced and verified experimentally at 1.37 GHz [2], was introduced in [4]. The Z antenna design incorporates a lumped element inductor that provides a simple means to tune its resonance frequency, particularly to lower frequencies. In this letter, we report the design and experimental verification of two Z antennas, one at 570 MHz and another at 300 MHz, which confirm the original design and performance characteristics [4].

The reported Z antenna designs and comparisons with experimental results were completed at the University of Arizona, Tucson. In all cases, these designs were tuned for operation at the desired frequency through Ansoft High Frequency Structure Simulator (HFSS) simulations (mention of this product is not an endorsement, but only serves to clarify the software used).

Manuscript received October 25, 2009. First published December 08, 2009; current version published December 22, 2009. This work was supported in part by DARPA Contract HR0011-05-C-0068. Part of this effort was U.S. government work, not subject to U.S. copyright.

R. W. Ziolkowski and P. Jin are with the Department of Electrical and Computer Engineering, University of Arizona, Tucson, AZ 85721-0104 USA (e-mail: ziolkowski@ece.arizona.edu).

J. A. Nielsen and M. H. Tanielian are with Boeing Research & Technology, Seattle, WA 98124-2499 USA.

C. L. Holloway is with the Electromagnetics Division, National Institute of Standards and Technology (NIST), Boulder, CO 80305 USA.

Color versions of one or more of the figures in this letter are available online at http://ieeexplore.ieee.org.

Digital Object Identifier 10.1109/LAWP.2009.2038180

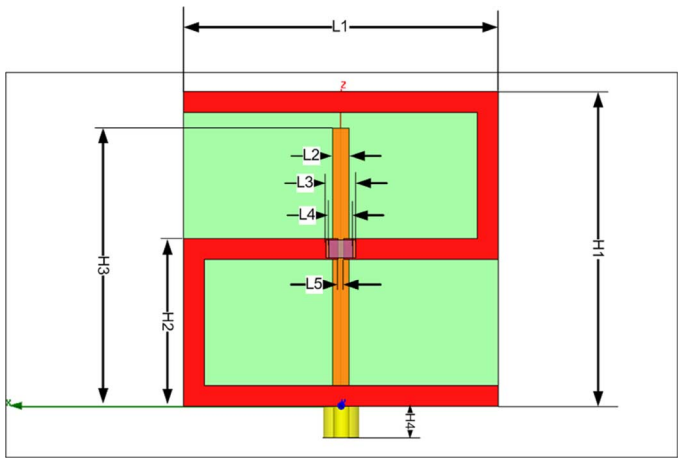

Fig. 1. The Z antenna and its design parameters: side view.

The fabrication and some preliminary measurements were completed at Boeing Research & Technology in Seattle, WA. All power efficiency measurements were carried out in the reverberation chamber (RC) at the National Institute of Standards and Technology (NIST) in Boulder, CO. The RC approach to measure the radiation efficiency of an antenna has been demonstrated to be a reliable alternative to the traditional Wheeler cap and anechoic chamber methods [5], [6].

II. Z Antenna Designs and Experiments

Because the air-suspended, thick copper Z antenna configuration suggested in [4] was experimentally found not to be mechanically robust, it was decided to redesign the Z antennas for fabrication with a Rogers Duroid 5880 substrate (identifying this product does not imply an endorsement, but only serves to specify the materials used). The relative permittivity and permeability of the 5880 material is 2.2 and 1.0, respectively, and the loss tangent is 9.0×10^{-4}.

As shown in Fig. 1, the redesigned Z antenna consists of a monopole that is printed on one side of a sheet of 0.5-oz (17-μm-thick copper), 31 mil (0.7874 mm) thick, 5880 material. It is coaxially fed through a finite-sized ground plane. The Z element is printed on the other side of the sheet; it consists of two "J" elements connected by a lumped element inductor. The size parameters for the Duroid-based Z antenna designs are noted in Fig. 1. The values $\mathrm{L2} = 1.5$ mm and $\mathrm{L5} = 0.5$ mm are common to all the designs reported here. For the 570 MHz versions, the parameter values were $\mathrm{L1} = 30$ mm, $\mathrm{L3} = 2.89$ mm,

TABLE I
Z ANTENNA DESIGN PARAMETERS (mm)

Design	L1	L3	L4	H1	H2	H3	ka
570.4 MHz Lossy Ind.	30	2.89	2.29	30	14	24.6	0.401
294.1 MHz Adjusted	40	8.58	7.98	40	21	26	0.276
285.6 MHz High Eff.	64	8.58	7.98	64	29	64	0.428

$\mathrm{L4} = 2.29$ mm, $\mathrm{H1} = 30$ mm, and $\mathrm{H2} = 14$ mm. The design parameters unique to each design are summarized in Table I.

For both design frequencies, Coilcraft inductors were used. For the 570-MHz case, the 47-nH inductor, part no. CoilCraft 1008HQ-47NX_L, was used [7]; for the 300-MHz case, the 169-nH Maxi inductor, part no 132-12SM_L, was used [8]. The coax center conductor diameter matched the thickness of the monopole; thus, its radius was $\mathrm{r_{inner}} = \mathrm{L2}/2 = 0.75$ mm and, consequently, its outer radius was $\mathrm{r_{outer}} = 2.301\ \mathrm{r_{inner}} = 1.726$ mm. This center conductor was extruded above the ground plane and then soldered directly to the monopole. The length of the coax, $\mathrm{H4} = 3$ mm, was used in all of the HFSS simulation models.

During fabrication, the inductor was mounted on the surface of the middle strip of the Z structure. In the HFSS simulations, the inductor was composed of a supporting lossless medium whose relative permittivity and permeability were 2.2 and 1.0, respectively; a rectangular *LRC* element; and two perfect electric conductor (PEC) ends connected to the *LRC* element. The *LRC* sheet is parallel to the *zx* plane and in the middle of the supporting medium. When losses are included, this rectangular sheet is divided into two equal parts in series, one representing the inductance and the other representing the resistance of the component. The inductance value is specified by the data sheet of the actual component. The losses are estimated from the circuit Q value charts given by the manufacturer. Without the PEC ends, the inductor length in the *x*-direction is L4, while with the PEC ends, it is L3. The depth of the inductor in the *y*-direction is 1.52 mm. The height of the inductor along the *z*-direction is 1.73 mm.

The 570-MHz, 30×30 mm^2, 47-nH inductor design was tested first. Two versions were fabricated. One treated the 47-nH inductor as lossless; the second treated it with a resistance of 1.62 Ω, based on the circuit Q value, 105 at 550 MHz, extracted from the manufacturer's data sheets. The HFSS simulations predicted nearly complete matching to the 50-Ω source at the resonance frequency $\mathrm{f_{res}} = 581.32$ MHz ($|\mathrm{S_{11}}| = -34.2$ dB) with the monopole length $\mathrm{H3} = 20$ mm in the ideal, lossless design; and at the resonance frequency $\mathrm{f_{res}} = 570.38$ MHz ($|\mathrm{S_{11}}| = -39.8$ dB) with $\mathrm{H3} = 24.6$ mm in the lossy design. For the lossless case, the corresponding electrical size was $\mathrm{ka} = 0.409$. The HFSS-predicted overall efficiency (OE, ratio of the total radiated to input power) was $\mathrm{OE} = 91.8\%$. The ratio of the half-power VSWR Q value to the Chu limit ($Q_{\mathrm{Chu}} = \eta_{\mathrm{rad}}[1/\mathrm{ka} + 1/(\mathrm{ka})^3]$, where η_{rad} is the radiation efficiency and a is the radius of the smallest enclosing sphere) [9] was $\mathrm{Q_{ratio,Chu}} = 8.4$. Relative to the more realistic Thal limit [10] it was $\mathrm{Q_{ratio,Thal}} = 5.6$. For the lossy case, the corresponding electrical size was $\mathrm{ka} = 0.401$. The HFSS-predicted overall efficiency was $\mathrm{OE} = 49.7\%$, and the Q ratios remained the same.

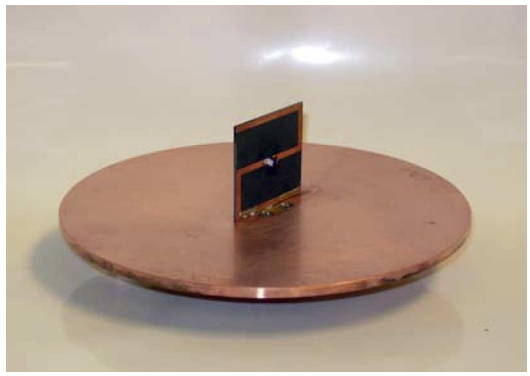

Fig. 2. Fabricated 570-MHz Z antenna on its small circular copper insert.

The Z antennas were fabricated with a small (120.6-mm-diameter copper plate) ground plane as shown in Fig. 2. They were then inserted into a larger ($18\ \mathrm{in} \times 18\ \mathrm{in} = 457.2 \times 457.2\ \mathrm{mm}^2$) copper ground plane (or not) for the *RC* measurements. A coaxial, panel mount connector was attached to the back of the small ground plane. The dielectric of the coax protruded slightly above the ground plane and caused the bottom portion of the Z element not to lie flush on the ground plane. The Z element was laser-welded to it in two spots. Two monopole antennas were also fabricated and tested to provide reference values. One was a wire monopole obtained by extending the center conductor of the coax to 25 mm above the ground plane to be approximately the same size as the printed monopole of the lossy 570-MHz Z antenna. The second was a 30-mm version that was the same length as the height of the lossy 570-MHz Z antenna and larger than the monopole length of the 300-MHz Z antenna.

The reverberation chamber was $2.8 \times 3.1 \times 4.6$ m^3 in size for the antenna characterization (see [11] for an overview of reverberation chambers and their applications). The NIST chamber used two rotating paddles in order to reduce the uncertainties in the measurements to 1.0 dB or less [12]. All power measurements were made relative to a reference antenna, an ETS LINGREN 3106 double-ridged waveguide horn that is about 94% efficient in its 200 MHz–2 GHz frequency band. A visual comparison of the small ground plane Z antenna and the reference dual-ridge horn antenna is shown in Fig. 3. The measured values of the magnitude of $\mathrm{S_{11}}$ and of the relative total radiated power for the various Z antennas are given in Figs. 4 and 5, respectively. The relative total radiated power for the bare 25-mm monopole (with no matching network) is also given in Fig. 5. It is about 30 dB below that of the Z antenna. This particular comparison was performed to confirm that, as predicted, the metamaterial-inspired near-field resonant parasitic acts as an internal matching network, which produces nearly complete matching to the source, and enhances the total radiated power by acting as a transducer, which changes the reactive field of the driven element into a propagating field.

Fig. 3. Comparison of the 570-MHz small ground plane Z antenna and the dual-ridged reference horn in the NIST–Boulder reverberation chamber.

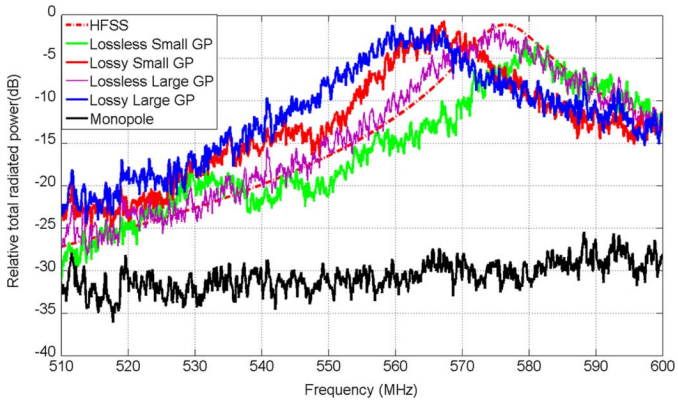

Fig. 5. Comparison of the relative total radiated power of the 570-MHz Z antennas in their small and large ground plane configurations and the large ground plane 25-mm bare monopole with no external matching network.

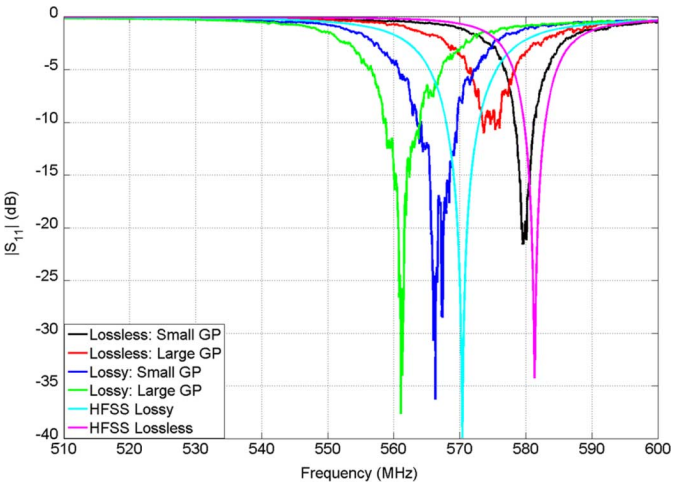

Fig. 4. HFSS-predicted and measured $|S_{11}|$ values for the two 570-MHz Z antennas in their small and large ground plane configurations.

Both of the fabricated Duroid-based 570-MHz Z antennas were measured in the small and large ground plane configurations. Note that the large ground plane versions were measured both in the center of the chamber and on the wall of the chamber, yielding essentially the same results. The small ground plane versions were measured in the center of the chamber. We note that the center-of-the-chamber antenna-under-test (AUT) measurements were also performed with several other cable layouts to confirm that the cable was not contributing to the measured total radiated power. These included loading the cable with a variety of ferrite beads at numerous different cable locations. The chamber-wall AUT measurements eliminated this issue since the cable was located in its exterior. The predicted and measured $|S_{11}|$ values in Fig. 4 show good agreement among all of the results. Nonetheless, the lossy design exhibited $|S_{11}|$ characteristics that were closer to the experimentally measured values.

The best measured total radiated power results (using the 94% efficiency value for the reference horn) were for the lossy small ground plane Z antenna: OE $=$ 80.0% (relative value $=-0.70$ dB) at 566.2 MHz (ka $=0.398$), 3 dB fractional bandwidth FBW $=$ 3.0%, and $Q_{\text{ratio,Chu}} = 4.03$. The corresponding results for the large ground plane lossy Z antenna were: OE $=$ 73.4% (relative value $=-1.12$ dB) at 561.05 MHz (ka $=$ 0.394), FBW $=$ 2.9%, and $Q_{\text{ratio,Chu}} = 4.35$. For the lossless, small ground plane case: OE $=$ 48.9% (relative value $=-2.84$ dB) at 579.5 MHz (ka $=$ 0.407), FBW $=$ 1.6%, and $Q_{\text{ratio,Chu}} = 11.89$. For the large ground plane case: OE $=$ 75.4% (relative value $=-0.96$ dB) at 561.05 MHz (ka $=0.394$), FBW $=$ 2.1%, and $Q_{\text{ratio,Chu}} = 6.31$. Consequently, these results show that the inductor loss is actually much less than the maximum predicted value, but definitely not zero. In fact, it was found that the best fit to the results came from a HFSS simulation with the resistance of the inductor being 0.35 Ω, which is about one-quarter of the maximum loss value. These HFSS-predicted relative total radiated power values are given in Fig. 5. With this resistance value, the HFSS-predicted overall efficiency was thus 79.6% (relative value $=-0.72$ dB) at 576.44 MHz ($|S_{11}| = -35.6$ dB), in very good agreement with the best measured value. The measured results show three important behaviors: 1) the resonances are in very good agreement with their predicted values; 2) the resonances persist even with a small ground plane, i.e., the size of the ground plane has a relatively small impact on the efficiency of the Z antenna when it is well designed; and 3) the loss based on the circuit Q of the inductor should be reduced for more accurate predictions of the design and for improved measured results.

Since patterns are not available from reverberation chamber measurements, the HFSS-predicted gain patterns for the large and infinite (wall-mounted) ground plane (GP) cases at the predicted resonance frequency are shown in Fig. 6 for completeness. These electric monopole type patterns show the expected impact of the ground plane size. The maximum gain is 1.61 dB at $\theta = 47^\circ$ for the finite GP version and 4.1 dB at $\theta = 90^\circ$ for infinite GP version.

The resonant frequency of the Z antenna [4] is given by the expression $f_0 = 1/\sqrt{L_{\text{eff}} C_{\text{eff}}}$, where L_{eff} and C_{eff} are the effective inductance and capacitance of the system. It has been found that the inductance value of the lumped element inductor dominates the effective inductance. Consequently, one can scale the antenna design to other frequencies simply by changing these effective values, particularly that of the lumped element. To

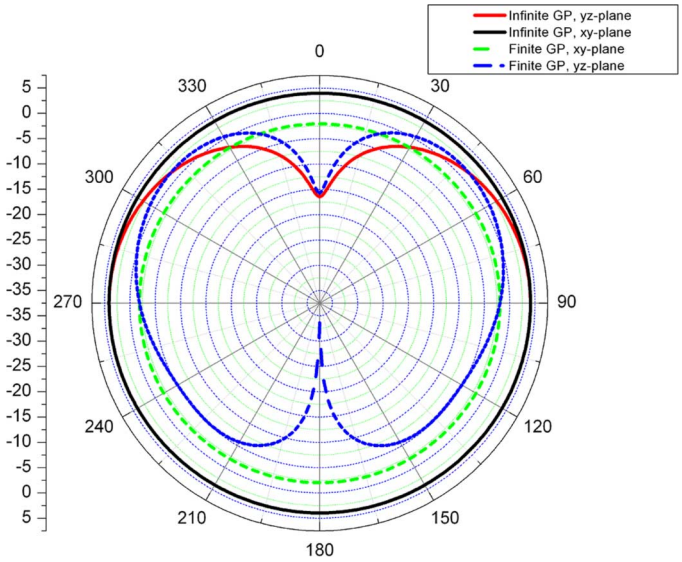

Fig. 6. HFSS-predicted patterns for the Z antenna at 576.44 MHz have the expected electric monopole shapes.

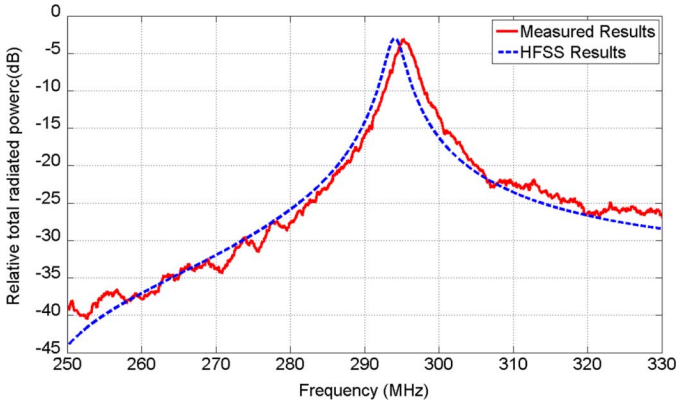

Fig. 7. Comparison of the HFSS predicted and measured relative total radiated power of the 300-MHz Z antenna.

demonstrate this capability, we redesigned the Z antenna with a larger inductor value for operation at 300 MHz.

The design parameters for the 300-MHz Z antenna were $\mathrm{L1} = 40$ mm, $\mathrm{L3} = 8.58$ mm, $\mathrm{L4} = 7.98$ mm, $\mathrm{H1} = 40$ mm, $\mathrm{H2} = 21$ mm, and $\mathrm{H3} = 34$ mm. For the HFSS simulations, the depth of the Maxi inductor in the y-direction was 5.97·mm, and its height along the z-direction was 5.74 mm. The HFSS-predicted values for this 40×40 mm^2 design with the 169-nH inductor were: $\mathrm{f_{res}} = 294.06$ MHz ($|\mathrm{S_{11}}| = -47.37$ dB) giving $\mathrm{ka} = 0.276; \mathrm{OE} = 23.3\%$ (assuming $\mathrm{R_{ind}} = 2.12\ \Omega$, based on the inductor circuit Q value); and $\mathrm{Q_{ratio,Chu}} = 7.6$ and $\mathrm{Q_{ratio,Thal}} = 5.1$. Because the Maxi inductor was physically much larger than the 47-nH inductor, its footprint was not an exact match to the trace widths, which were the same as the 570-MHz design. Consequently, the 300-MHz Z antenna had to be fabricated with the inductor tilted to enable good soldering contacts to the traces. Moreover, because the coax dielectric still protruded slightly above the ground plane, gold foil was attached between the bottom horizontal trace of the Z element and the ground plane, in addition to the two laser welds, in order to achieve a better contact with the ground plane.

This 300-MHz Z antenna was tested in the new NIST reverberation chamber, which is $2.95 \times 3.63 \times 4.27$ m^3 in size. Initial measurements showed poor matching to the source. The height of the monopole was then adjusted incrementally to 26 mm, where good matching ($|\mathrm{S_{11}}| = -27.16$ dB) was achieved again at $\mathrm{f_{res}} = 294.06$ MHz. The relative total radiated power measurements are shown in Fig. 7. It was found that the peak value was -3.1 dB, giving a measured overall efficiency $\mathrm{OE} = 46.0\%$. Adjusting the height of the monopole to $\mathrm{H3} = 26$ mm, the HFSS-predicted overall efficiency was $\mathrm{OE} = 47.5\%$ at the resonance frequency when the resistance of the inductor was lowered to 0.7 Ω, about one-third of the maximum circuit Q-based loss value. The relation between the real loss and the maximum predicted loss is less than the previous case because the Maxi element is an air core inductor, which gives it a higher circuit Q-based value and, hence, a lower resistance value. The design parameters for this adjusted design are summarized in Table I. A comparison of the HFSS-predicted and the measured relative total radiated power values is given in Fig. 7. Very good agreement between all of the simulated and measured results is observed.

Finally, for further comparisons, the relative total radiated power of the large ground plane 30-mm monopole antenna was measured with and without an external matching network. A MFJ-902H Travel Tuner was used to provide matching ($|\mathrm{S_{11}}| \sim -33$ dB) to the source at the Z antenna resonance frequency. The measured results for the bare and the matched monopole were, respectively, less than or equal to -35 and -22 dB over the same frequency range shown in Fig. 7. Even though its electrical size with the matching network is much larger than the Z antenna, the matched monopole had a relative total radiated power that was more than 20 dB less than the Z antenna values near the resonance frequency.

III. Conclusion

We have demonstrated that the electrically small Z antenna performs as predicted at 570 and 300 MHz. Nearly complete matching with no external matching circuit was achieved in both cases. Reasonable agreement between the predicted and measured total radiated power values was demonstrated. Direct comparisons with a comparable monopole antenna with and without an external matching network were also reported. The Z antennas, with no matching network, were measured to be much more efficient than an externally matched monopole antenna of a similar size.

One major goal of these designs and experiments was to achieve a better understanding of how to model the lumped element inductor in such near-field resonant parasitic antenna designs. Using the measured 300-MHz Z antenna results, a more efficient design has been obtained. In particular, the original design was changed to one with $\mathrm{L1} = 64$ mm, $\mathrm{H1} = 64$ mm, $\mathrm{H2} = 29$ mm, $\mathrm{H3} = 60$ mm, and a CoilCraft 90-nH Maxi inductor. These values are also summarized in Table I. Adjusting the resistance of the inductor to one-third of its circuit-Q (200 at 300 MHz) predicted value, $\mathrm{R_{ind}} = 0.2827\ \Omega$. The HFSS-predicted overall efficiency is $\mathrm{OE} = 82.3\%$ at $\mathrm{f_{res}} = 285.6$ MHz

($|S_{11}| = -25.44$ dB). We hope to fabricate and test this experimentally influenced $ka = 0.428$ Z antenna design with the parasitic element flush mounted to the ground plane, giving us the best opportunity to achieve this predicted, enhanced high-efficiency result.

REFERENCES

[1] R. W. Ziolkowski and A. Erentok, "Metamaterial-based efficient electrically small antennas," *IEEE Trans. Antennas Propag.*, vol. 54, no. 7, pp. 2113–2130, Jul. 2006.

[2] A. Erentok and R. W. Ziolkowski, "Metamaterial-inspired efficient electrically small antennas," *IEEE Trans. Antennas Propag.*, vol. 56, no. 3, pp. 691–707, Mar. 2008.

[3] R. W. Ziolkowski, C.-C. Lin, J. A. Nielsen, M. H. Tanielian, and C. L. Holloway, "Design and experimental verification of a 3D magnetic EZ antenna at 300 MHz," *IEEE Antennas Wireless Propag. Lett.*, vol. 8, pp. 989–993, 2009.

[4] R. W. Ziolkowski, "An efficient, electrically small antenna designed for VHF and UHF applications," *IEEE Antennas Wireless Propag. Lett.*, vol. 7, pp. 217–220, 2008.

[5] N. Serafimov, P.-S. Kildal, and T. Bolin, "Comparison between radiation efficiencies of phone antennas and radiated power of mobile phones measured in anechoic chambers and reverberation chamber," in *Proc. IEEE Antennas Propag. Int. Symp.*, San Antonio, TX, Jun. 16–21, 2002, vol. 2, pp. 478–481.

[6] G. Le Fur, C. Lemoine, P. Besnier, and A. Sharaiha, "Performances of UWB Wheeler cap and reverberation chamber to carry out efficiency measurements of narrow band antennas," *IEEE Antennas Wireless Propag. Lett.*, vol. 8, pp. 332–335, 2009.

[7] *Coilcraft*, [Online]. Available: http://www.coilcraft.com/1008hq.cfm

[8] *Coilcraft*, [Online]. Available: http://www.coilcraft.com/maxi.cfm

[9] L. J. Chu, "Physical limitations of omni-directional antennas," *J. Appl. Phys.*, pp. 1163–1175, 1948.

[10] H. Thal, "New radiation Q limits for spherical wire antennas," *IEEE Trans. Antennas Propag.*, vol. 54, no. 10, pp. 2757–2763, Oct. 2006.

[11] C. L. Holloway, D. A. Hill, J. M. Ladbury, P. Wilson, G. Koepke, and J. Coder, "On the use of reverberation chambers to simulate a controllable Rician radio environment for the testing of wireless devices," *IEEE Trans. Antennas Propag.*, vol. 54, no. 11, pp. 3167–3177, Nov. 2006.

[12] D. A. Hill and M. Kanda, "Measurement uncertainty of radiated emission," NIST, Boulder, CO, Tech. Note. 1389, 1997.